04 - EFFECT OF TRENDS ON REGIONAL FLOOD FREQUENCY GROWTH CURVE AND AT-SITE QUANTILE ESTIMATES

Uzzal Mandal[1], Conleth Cunnane[2], Brendan Brice[1]

[1] *RPS Consulting Engineers*
[2] *University of Galway (retired)*

Abstract

It was intuitively felt that the flood quantiles estimated from data series that contain an upward trend would be larger than those estimated from trend free data. However, judgement about the effects of trends on the flood growth factors [$X(T) = Q(T)/Q^{'}$] is not so clearcut since the denominator of the growth factor might also be affected by the trend. The effects of trends on the regional growth curves and at-site flood quantiles were investigated through Monte Carlo Simulation techniques and using the Hosking and Wallis (1997) proposed L-moment algorithm procedures. Two different linear forms of trends were applied to the data series, one was in additive and the other was in hybrid (both additive and multiplicative) form referred to as TF-1 and TF-2 respectively. Four different true and fitted distribution combinations were used for generating and fitting the data series respectively i.e. GEV-GEV, GEV-EV1, EV1-EV1 & EV1-GEV. Model simulations were carried out for 10,000 realisations of pooling regions with each region comprising 15 sites with 30 years of records at each site giving a total pooled record of 450 station-years in each realisation. The simulation results showed that the presence of any trend in data series causes changes in the distribution parameters, depending on the form and magnitude of trend and type of true distribution. TF-1 generally causes a flattening of growth curves, while TF-2 has the opposite effect. The change in growth factor can be as large as 16% for 100-year flood event at a trend slope of 1%. Trend effect on quantiles is also generally positive, largely caused by an increase in the index-flood, with increases up to 17% for 100-year flood event at a trend slope of 1%. The increase rate in the flood quantiles may not be noticeable for a very small trend slope (<0.2%). However, for larger trend slopes (>0.2%) the effects could be more significant and may impact project safety and cost. In this context careful attention should be given in estimating the design flood quantiles where non-stationarity properties exist in the data.

1. INTRODUCTION

In statistical flood frequency analysis, the key assumptions are that all observations in a data series are independent and identically distributed (IID), i.e. the data series are stationary. In the context of climate change, however, it is possible that these assumptions may no longer be valid. The parameters describing the location, scale and shape properties of hydrological time series may change over time and as a result data series may become non-stationary. The violations to the IID assumptions could occur due to changes in streamflows caused either directly by human interventions or from long-term climate change and climate variability caused by the atmospheric circulations (ENSO, PDO and NAO phenomena). The evidence of global average temperature change (increases) was confirmed in the climate change reports prepared by the Intergovernmental Panel on Climate Change (IPCC) (1996, 2001, 2007, 2014 and 2021). This increase in temperature has caused changes in climate parameters, such as precipitation and evapotranspiration which in turn have impacted the frequency and magnitude of streamflows. The climatic changes can impact streamflow time series gradually (a trend) or abruptly (a step change).

The results of trend tests carried out on the Irish Annual Maximum Flood (AMF) series in the FSU Research (OPW, 2012) concluded that the Irish flood series exhibit more non-stationarity (i.e. trends and step changes) than would be expected by chance. Significant trends were identified at 30% of sites (28 out of 93 sites) at 5% significance level. This obviously casts doubt on the validity of the IID assumptions.

The application of the conventional statistical flood frequency technique on such non-stationary data series would result in under- and/or over-estimation of a design flood quantile.

The presence of a trend has a considerable effect on the interpretation of results when fitting a probability distribution to a sample of non-stationary observations. In engineering hydrology overestimating the design values as a result of ignoring significant decreasing trends in the data series may lead to over designed projects and the associated unnecessary increased capital costs. The more serious cases arise from ignoring increasing trends in flood series, which may lead to under designed projects and significant losses when more severe floods occur than are expected. Cox et al. (2002) explored the effects of trend (linearly varying deterministic trend) in mean and dispersion on the distribution of extremes using a simple theoretical model (Gumbel distribution). The results showed that if a trend in location and/or scale parameter is likely, prediction of maxima on this basis of the projected parameter values at the midpoint of the planning horizon is slightly overoptimistic. Based on a non-stationary pooled flood frequency approach, Cunderlik and Burn (2003) showed that ignoring even a weakly significant non-stationarity in the data series (significant at 10% significance level) may seriously bias the quantile estimation for horizons as near as 0-20 years in the future.

Estimation of design flood flow under the non-stationary hypothesis is very complex. Frequency analysis of a non-stationary time series requires a different approach than the conventional stationary one because the distribution parameters and the distribution itself change over time and so do the estimates of exceedance probability and associated uncertainty of a design value of interest. Thus, any evidence of departure from basic assumptions of independence and stationarity of observations could significantly affect the validity of frequency analysis results (Porporato and Riodolfi, 1998; Cox et al., 2002; Cunderlik and Burn, 2003). Therefore, alternate approaches that incorporate the effects of non-independence and non-stationarity should be used and further developed and the assumption of IID in the data series should be considered only as a first approximation.

The non-stationary frequency analysis is a relatively new modelling approach and the number of studies is rather small but is continuously increasing, perhaps, because of the vulnerability of society and ecosystems to global climate changes predicted by the climate models (IPCC, 2007). North (1980) developed a time-dependent flood frequency model in which both the time of occurrence and the flood magnitude were time-dependent variables. Duckstein et al. (1987) outlined the Bayesian approach to the estimation of the posterior flood distribution. Strupczewski et al. (2001) and Strupczewski and Kaczmarek (2001) developed a non-stationary flood frequency procedure comprising 56 models of flood distribution and trend function. Cunderlik and Burn (2003) proposed a second order non-stationary approach to pooled flood frequency analysis by assuming at-site non-stationarity in the first two moments (i.e., mean and variance of the time series). Khaliq et al. (2006) provided an extensive review of the various existing approaches of non-stationary frequency analysis.

Until now no such acceptable and/or reliable procedure has been developed and/or adopted to deal with these non-stationary properties of data series. Furthermore, only a small number of studies so far have explored the effects of non-stationarity in the data series on the design flow estimates using the conventional flood frequency analysis techniques (Cox et al., 2002; Cunderlik and Burn, 2003, Khaliq et al., 2006). Further, the information extracted from limited length records of a small number of sites may not be representative of the regional behaviour and could lead to misdiagnosis (Jain and Lall, 2000; IPCC, 2001). Therefore, it is important to establish the significance of non-stationarity in the regional context, preferably using long observational records where available, using a suitable regional approach (e.g., see Burn and Hag Elnur, 2002 for such an approach). Satisfactory detection of consistent regional changes (increases/decreases) in the statistics of extremes, as compared to just site-specific ones, could be more interesting and useful for decision-making to revise design methodology or to plan adaptability to climate change.

The present study therefore focused on determining the effects of non-stationarity/trend on quantile estimates, particularly on the regional growth curves, at various degrees of trend conditions. It is considered that the non-stationarity in the AMF series would have resulted mainly from climate change impact on a regional basis. This trend effect assessment has therefore been focused on a regional scale basis rather than on a single site basis. The findings of this study would help hydrologists to make an allowance in the estimated design flood based on the conventional flood frequency analysis technique.

2. METHODOLOGY

The study was carried out using a Monte Carlo Simulation technique proposed by Hosking and Wallis (1997). Initially, the effect of trends on sample properties such as the first three sample moments (Mean, L-CV and L-Skewness) were investigated. Subsequently, any effects of trends on the distribution moments and parameters were examined. Finally, any changes in the estimates of regional growth curves and at-site quantiles (over the stationary condition) were investigated for various trend scenarios. It was considered reasonable that the non-stationarity in the AMF series would result mainly from climate change impact on a regional basis. This trend effect assessment was therefore focused on a regional scale basis rather than on a single site basis.

2.1 Selection of pooling group and random sample generation

A pooling group of size 450 station-year records consisting of 15 hydrologically similar sites, each with a record length of 30 years, was used. This was based on the findings of the sensitivity study carried out by Hosking and Wallis (1997). A moderately heterogeneous region (Hosking-Wallis, 1997) with L-CV and L-Skewness both linearly varying from 0.20 at site 1 to 0.30 at site 15 with a range of 0.10 was felt appropriate in the context of real world data. A true distribution mean of 1.0 was used.

In practical applications, the linear variation of L-moment ratios among the sites in a region will often be the case i.e. sites with high L-CV also tend to have high L-Skewness (Hosking and Wallis, 1997; Lu and Stedinger, 1992b). In the Irish Flood Studies Update (FSU) research, Das and Cunnane (2011) found that the most of the Irish pooling groups of AMF series exhibits a degree of heterogeneity among the group members, similar to the above-mentioned heterogeneity mentioned by Hosking and Wallis (1997) in their study. Four different combinations of floodlike distributions (extreme value type) were used for simulating and fitting the data to estimate the regional growth curve and quantiles for a range of return periods. These include:

(i) GEV-GEV: where both generation and fitting were carried out using the GEV distribution,
(ii) GEV-EV1: where true distribution is GEV and the fitted distribution is EV1,
(iii) EV1-EV1: where both generation and fitting were carried out using the EV1 (Gumbel) distribution, and
(iv) EV1-GEV: where random samples were generated from EV1 distribution and were fitted to GEV distribution.

The selection of GEV and EV1 distributions, in the context of Irish AMF Series, was based on the finding of a study carried out under the Irish Flood Studies Update (FSU) Programme (Das and Cunnane, 2011).

2.2 Application of Trends

The true form of trend in the historical time series is unknown, most likely it would be non-linear in nature. However, in order to simplify our understanding, a linear upward type trend model, which is easy to formulate mathematically, was considered in this study. It was assumed that the first moment of the sample's true distribution would be much more sensitive to the long-term climate change effect than the other higher order moments. Therefore, upward linear trend was applied to the sample mean. The

following two deterministic trend forms were employed to introduce trends in the stationary time series:

(i) Trend Form 1 (TF-1): $Q_{NS}(t) = Q_S(t) + T_S t$ (1)

(ii) Trend Form 2 (TF-2): $Q_{NS}(t) = Q_S(t)[1 + T_S t]$ (2)

where , $Q_{NS}(t)$ = non-stationary time series,
$Q_S(t)$ = stationary time series,
T_S = upward trend slope (per unit time step)
t = time step (year), 1 to 30 years

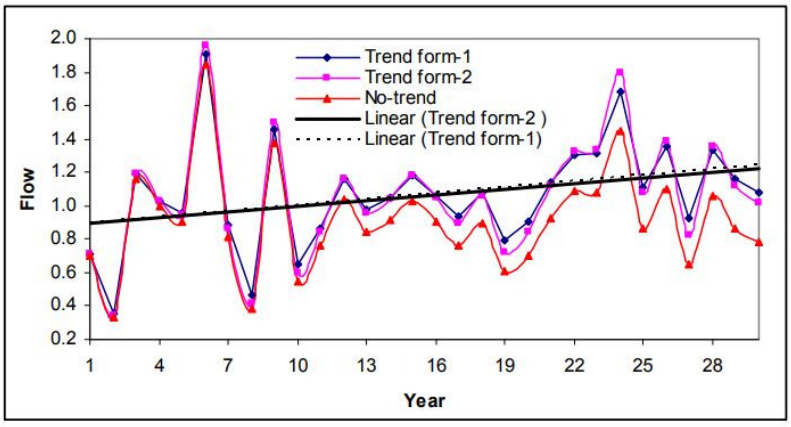

Figure 1: Graphical presentation of two different trend forms with 1% upward trend slope.

Trend Form 1 (linear model) is similar to those used by Lettenmaier, 1976 and Yue et al., 2002, while the TF-2 is a hybrid type model proposed in this current study. Figure 1 shows a graphical comparison of these two trend forms. The red line represents a sample of a stationary time series with 30 years record length, which were drawn from GEV distribution with mean, L-CV and L-Skewness of 1.0, 0.25 and 0.25 respectively. The blue and pink lines represent the corresponding non-stationary time series (derived through applying a 1% upward trend slope) for the TF-1 and TF-2 trend forms respectively. Changes in the time series magnitudes over the record lengths are visible in the plots. A linear regression trend line has been estimated for each of the non-stationary samples with different trend forms. It can be seen from these plots that the estimated slope of the regression line for TF-1 is slightly greater than that of TF-2. However, it can be seen that the TF-2 trend forms introduces more variability in the time series than the TF-1 trend form.

If the cause of trend in the data series is mainly believed to be the climate change, then it is reasonable to assume uniformity in trend magnitudes across the region (i.e. a fixed rate trend applies to all sites in the region). However, some degree of variability can be expected among the sites due to the regional variations in climate change and variability in the changes of soil moisture characteristics in their relevant catchments. The effect on the quantile estimate is believed to be minimal due to this variability. Based on this, the trend impact assessment was carried out for a spatially fixed rate of trend across the region. A range of upward trend slopes starting from 0% to 4% with an increment of 0.2% was applied homogeneously at all sites in the region. This trend slope range of 0% to 4% is based on the identified upward trend slopes in the Irish AMF series (Mandal U., 2011).

2.3 Growth Curve and At-site Quantile Estimation Methods

The at-site quantiles were estimated using the 'Index-flood and L-moment parameter estimation method' as recommended by Hosking and Wallis (1985a, 1993, 1997). The index-flood used in this study is the at-site sample mean.

2.4 Trend Effect Assessments

The presence of trend in flood records would cause changes (increase or decrease) in sample properties such as mean, L-CV and L-skewness, which could consequently result in under- or over-estimation of regional growth curve and quantile estimates. In assessing the effects of trends in the growth curve and quantile estimates, the Hosking and Wallis (1997) recommended Monte Carlo simulation method was used. In this procedure, a region was specified first, i.e. the number of sites and record length for each site. Data were then generated from a specified distribution (true distribution) for all sites in the region. Trend was then applied to these records. These records were then fitted by using a selected distribution and parameter estimation method. The estimated growth curves and at-site quantiles were compared with the true/no-trend values implied by the frequency distribution specified for each site, and the effects (increase or decrease) are calculated for each of the estimators (growth curves and at-site quantiles). This procedure was repeated for many realisations (M) of regions. The effects associated with any of the estimators were quantified in terms of relative bias/deviation, $B(F)$, relative root mean square error, $R(F)$ expressed as percentages. These were estimated by:

$$B_{i,s}(F) = \frac{1}{M}\sum_{m=1}^{M}\frac{\hat{Q}_{i,s}{}^{[m]}(F) - Q_i(F)}{Q_i(F)} \times 100\% \quad (3)$$

$$R_{i,s}(F) = \left[\frac{1}{M}\sum_{m=1}^{M}\left\{\frac{\hat{Q}_{i,s}{}^{[m]}(F) - Q_i(F)}{Q_i(F)}\right\}^2\right]^{1/2} \times 100\% \quad (4)$$

Where $B_{i,s}(F)$ = relative bias/deviation of site *i* quantile estimate of non-exceedance probability '*F*' for the trend slope magnitude '*s*'.

$R_{i,s}(F)$ = relative root mean square error of site *i* quantile estimate of non-exceedance probability '*F*' for the trend slope magnitude '*s*'.

$\hat{Q}_{i,s}{}^{[m]}(F)$ =estimated site *i* quantile estimate of non-exceedance probability '*F*' for the trend slope magnitude '*s*' under the mth realisation of the region (*m* = 1 to *M*; *M* is the number of realisations).

To obtain a summary of the changes of an estimate over all of the sites (*N*) in the region, the regional average values have been computed as follows:

Regional average relative bias/deviation for trend slope, s:

$$B^R{}_s(F) = \frac{1}{N}\sum_{i=1}^{N} B_{i,s}(F) \quad (5)$$

Regional average absolute relative bias/deviation for trend slope, s:

$$A^R{}_s(F) = \frac{1}{N}\sum_{i=1}^{N}\left|B_{i,s}(F)\right| \quad (6)$$

Regional average relative RMSE for trend slope, s:

$$R^R(F) = \frac{1}{N}\sum_{i=1}^{N} R_i(F) \quad (7)$$

For the no-trend condition (0% slope), the above-mentioned measures assess the performance of a distribution and their parameter estimation method in estimating an estimator. In any trend condition,

these measures would rather estimate the effect of trends on the true quantiles. For example, the bias terms, $B_{i,s}(F)$ and $B^R{}_s(F)$ would measures the relative differences (increases/decreases) in quantile estimates to be caused by various trend slope magnitudes at the at-site and regional levels respectively. For a particular trend scenario, $\hat{Q}_{i,s}(F)$ in equation (3) will be the quantile estimate associated with this trend slope, while $Q_i(F)$ will remain the true at-site quantile estimate under all realisations.

3. RESULTS AND DISCUSSIONS

Initially the impacts of trends on the sample properties such as the first three moments - Mean, L-CV and L-skewness, were investigated. Subsequently, the changes in the distribution parameters were examined. Finally, any changes in the estimates of regional growth curves and at-site quantiles (over the stationary condition) were investigated for various trend scenarios. Model simulations were carried out for 10,000 realisations of regions (M = 10,000). The changes in distribution properties and quantile values were calculated with respect to the true values on a regional scale basis. The region is specified earlier in section 2.1. The true values of at-site L-moment ratios, distribution parameters and the at-site true quantile estimates for all sites in the region including the regional growth factors for a range of non-exceedance probabilities (F) are given in Tables 1 and 2 (for the GEV and EV1 distributions respectively). The regional growth curve has been calculated from the harmonic mean of the at-site quantile estimates in each case.

Table 1: True at-site properties, distribution parameters and at-site quantile values for GEV distribution (reproduced from Hosking and Wallis, 1993; the mean of all distribution is 1.0).

Site	L-CV	L-Skew.	n_i	GEV Parameters			True at-site Quantiles							
				u	alpha	k	F=0.010	0.100	0.500	0.800	0.900	0.950	0.990	0.999
1	0.200	0.200	30	0.828	0.276	-0.046	0.421	0.602	0.930	1.256	1.482	1.706	2.242	3.073
2	0.207	0.207	30	0.820	0.283	-0.057	0.407	0.590	0.925	1.263	1.499	1.735	2.307	3.213
3	0.214	0.214	30	0.812	0.289	-0.068	0.393	0.578	0.920	1.269	1.516	1.764	2.374	3.361
4	0.221	0.221	30	0.805	0.296	-0.079	0.379	0.566	0.915	1.275	1.532	1.793	2.442	3.514
5	0.229	0.229	30	0.797	0.302	-0.089	0.366	0.555	0.909	1.281	1.549	1.823	2.512	3.677
6	0.236	0.236	30	0.789	0.307	-0.100	0.354	0.543	0.904	1.286	1.565	1.852	2.584	3.846
7	0.243	0.243	30	0.781	0.313	-0.110	0.341	0.532	0.898	1.292	1.581	1.882	2.658	4.025
8	0.250	0.250	30	0.773	0.318	-0.121	0.329	0.521	0.893	1.297	1.597	1.911	2.732	4.210
9	0.257	0.257	30	0.765	0.324	-0.131	0.318	0.510	0.887	1.302	1.612	1.940	2.809	4.403
10	0.264	0.264	30	0.757	0.329	-0.142	0.306	0.499	0.881	1.306	1.628	1.970	2.888	4.608
11	0.271	0.271	30	0.749	0.333	-0.152	0.295	0.488	0.875	1.311	1.643	2.000	2.968	4.820
12	0.279	0.279	30	0.741	0.338	-0.162	0.284	0.478	0.869	1.315	1.658	2.030	3.051	5.045
13	0.286	0.286	30	0.733	0.342	-0.173	0.274	0.467	0.862	1.318	1.673	2.060	3.134	5.277
14	0.293	0.293	30	0.725	0.346	-0.183	0.264	0.457	0.856	1.322	1.688	2.090	3.220	5.522
15	0.300	0.300	30	0.717	0.350	-0.193	0.254	0.447	0.849	1.325	1.702	2.119	3.307	5.775
Regional growth curve (harmonic mean)							**0.325**	**0.518**	**0.891**	**1.294**	**1.592**	**1.903**	**2.711**	**4.137**

Table 2: True at-site properties, distribution parameters and at-site quantile values for EV1 distribution

Site	L-CV	L-Skew.	n_i	EV1 Parameters		True at-site Quantiles							
				u	Alpha	F=0.010	0.100	0.500	0.800	0.9	0.95	0.99	0.999
1	0.200	0.200	30	0.834	0.289	0.393	0.593	0.939	1.266	1.483	1.690	2.161	2.826
2	0.207	0.207	30	0.828	0.299	0.371	0.578	0.937	1.276	1.500	1.715	2.202	2.892
3	0.214	0.214	30	0.822	0.309	0.349	0.564	0.935	1.285	1.517	1.740	2.244	2.957
4	0.221	0.221	30	0.816	0.320	0.328	0.549	0.933	1.295	1.534	1.764	2.285	3.022
5	0.229	0.229	30	0.810	0.330	0.306	0.535	0.931	1.304	1.552	1.789	2.327	3.087

6	0.236	0.236	30	0.804	0.340	0.284	0.520	0.928	1.314	1.569	1.814	2.368	3.153
7	0.243	0.243	30	0.798	0.350	0.263	0.506	0.926	1.323	1.586	1.838	2.410	3.218
8	0.250	0.250	30	0.792	0.361	0.241	0.491	0.924	1.333	1.603	1.863	2.451	3.283
9	0.257	0.257	30	0.786	0.371	0.219	0.476	0.922	1.342	1.621	1.888	2.492	3.348
10	0.264	0.264	30	0.780	0.381	0.198	0.462	0.920	1.352	1.638	1.912	2.534	3.414
11	0.271	0.271	30	0.774	0.392	0.176	0.447	0.917	1.361	1.655	1.937	2.575	3.479
12	0.279	0.279	30	0.768	0.402	0.154	0.433	0.915	1.371	1.672	1.962	2.617	3.544
13	0.286	0.286	30	0.762	0.412	0.133	0.418	0.913	1.380	1.690	1.986	2.658	3.609
14	0.293	0.293	30	0.756	0.423	0.111	0.404	0.911	1.390	1.707	2.011	2.700	3.674
15	0.300	0.300	30	0.750	0.433	0.089	0.389	0.909	1.399	1.724	2.036	2.741	3.740
Regional growth curve (harmonic mean)						**0.199**	**0.483**	**0.924**	**1.332**	**1.600**	**1.857**	**2.438**	**3.259**

3.1 Changes in Sample Properties

Changes in the sample properties such as mean, L-CV and L-Skewness with the increases in trend slopes were examined for different combinations of trend forms and true distribution types. It was found that the regional average 'mean' changes in a similar fashion for both trend forms and distribution types. It increases linearly with the increase in trend slopes at the same rate in both distributions and trend forms [Figures 2(a) & 2(b)]. However, the patterns of changes in L-CV and L-Skewness are different in different trend forms. The regional average L-CV and L-Skewness decrease in the case of TF-1, while they increase in the TF-2 case with the increase in trend slopes. The changing rates are markedly larger in TF-1 than TF-2. These are true in both EV1 and GEV distributions [Figures 2. (c), (d), (e) & (f)]. Table 3 presents the changes in regional average mean, L-CV & L-Skewness for 1% trend increase for both trend forms and distribution types (GEV and EV1).

Table 3: Changes in regional average mean, L-CV & L-Skewness for 1% trend increase for both trend forms and distribution types (GEV and EV1).

Trend slope	GEV distribution						EV1 distribution					
	Mean		L-CV		L-Skewness		Mean		L-CV		L-Skewness	
	TF-1	TF-2	TF-1	TF-2	TF-1	TF-2	TF-1	TF-2	TF-1	TF-2	TF-1	TF-2
0.0%	1.000	1.000	0.248	0.248	0.237	0.237	1.000	1.000	0.250	0.250	0.164	0.164
1.0%	1.155	1.155	0.220	0.252	0.222	0.239	1.155	1.155	0.221	0.253	0.153	0.168

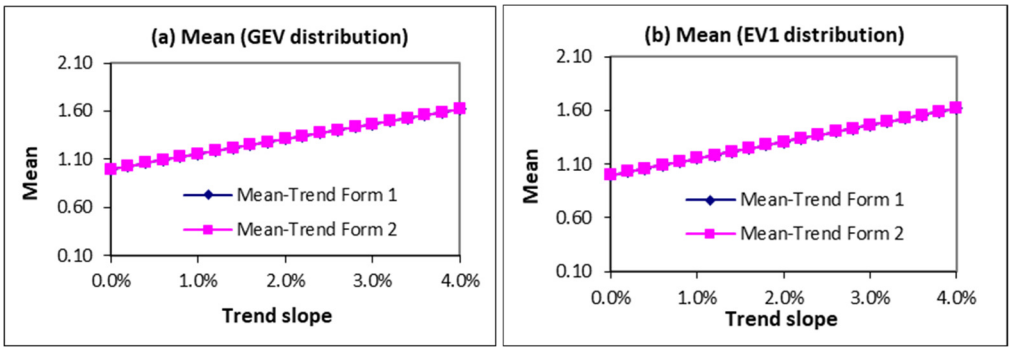

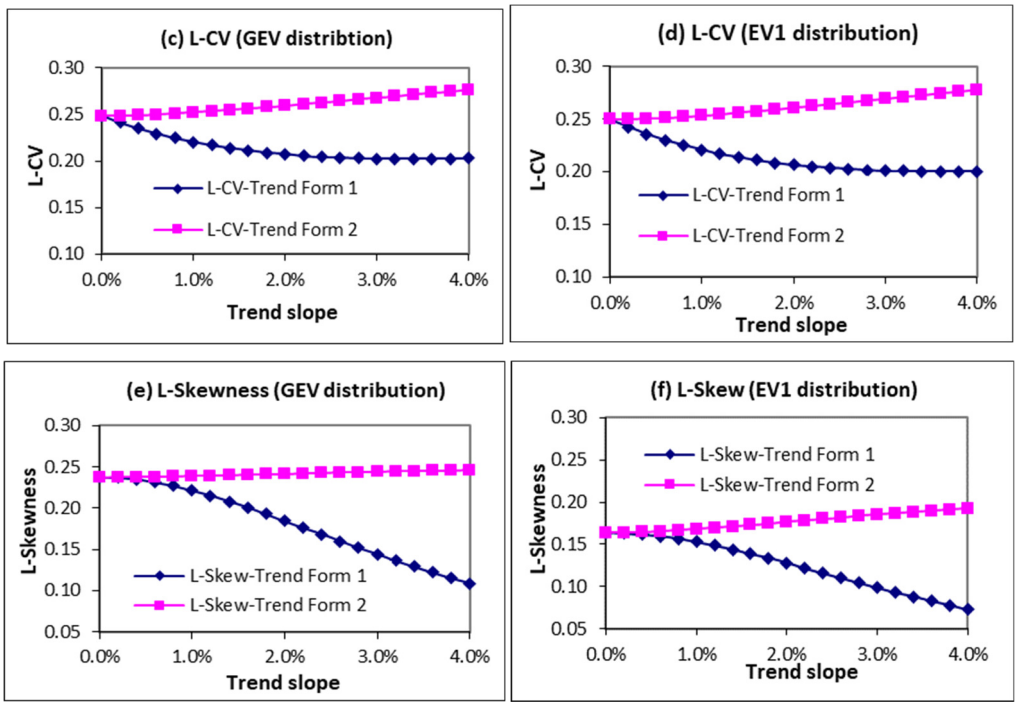

Figure 2: Comparison of the changes in regional average mean, L-CV & L-skewness with the increase in trend slopes for both trend forms

An examination of the L-moment ratio diagram for all trend scenarios showed that the sites with larger at-site L-CVs are more sensitive to trend slopes, i.e. their L-CV values decreases more than that of the sites with lower L-CVs with the increase in TF-1 type trend slope [Figure 3(a)]. In contrast, in the TF-2 case, the at-site L-CVs increases almost at an equal rate in all sites in the region [Figure 3(b)]. This explains why the regional average L-CV value decreases with the trend slope in the case of TF-1 and increases in TF-2. Figure 3(a) & 3(b) also show the rate of changes in the at-site L-Skewness with the increase in trend slope are almost equal at all sites in the region. TF-1 reduces at-site L-Skewness, while TF-2 inflates it. The change rate is higher in the TF-1 case than in TF-2. Due to these changes in at-site L-Skewness, regional average L-Skewness decreases in TF-1 and increases in TF-2. This analysis thus suggests that TF-1 reduces the variability and asymmetry while TF-2 inflates these properties (Table 3). The subject properties are found to be more sensitive to TF-1 than that to TF-2. These two scenarios are opposite; however, both could occur in the real world due to the changing climate and/or due to any anthropogenic changes in the catchment characteristics.

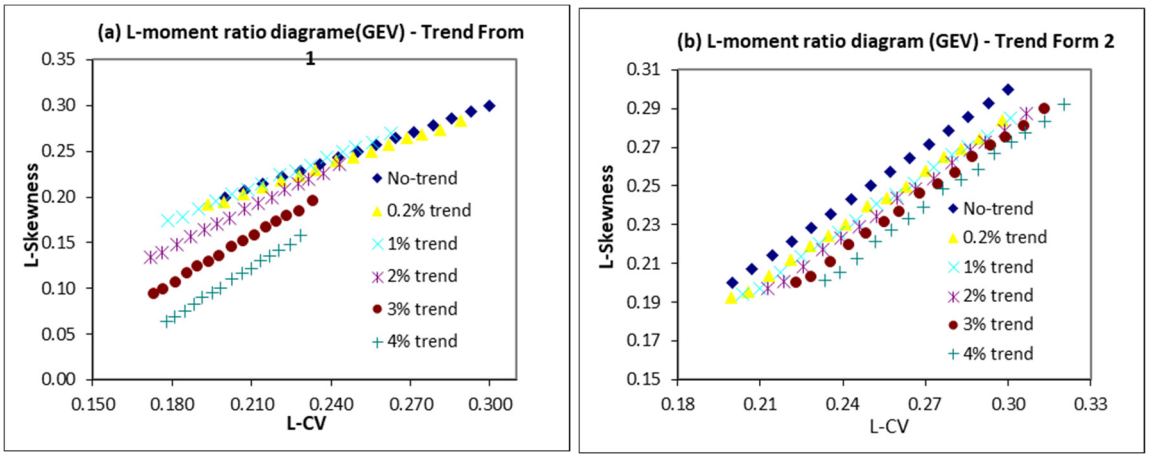

Figure 3: L-moment ratios for all sites in the region for different trend scenarios and forms (samples were generated from GEV distribution)

3.2 Changes in Distributions Parameters

Changes in distribution parameters for both EV1 and GEV distributions with the increase in trend slopes were investigated for both trend forms. The changes in sample properties caused changes in the distribution parameters. In the case of GEV distribution, the patterns of changes in the location and scale parameters are similar in both cases of trend forms, i.e. they both increase with the increase in trend slopes [Figure 4(a) & 4(b)]. A slightly larger increase in scale parameter in TF-2 was noticed. This was expected as TF-2 introduced more variability in the data series. The shape parameter increases with the increase in trend slopes in the case of TF-1, while it decreases in the TF-2 case. The changing rate is markedly higher in the case of TF-1 [Figure 4(c)].

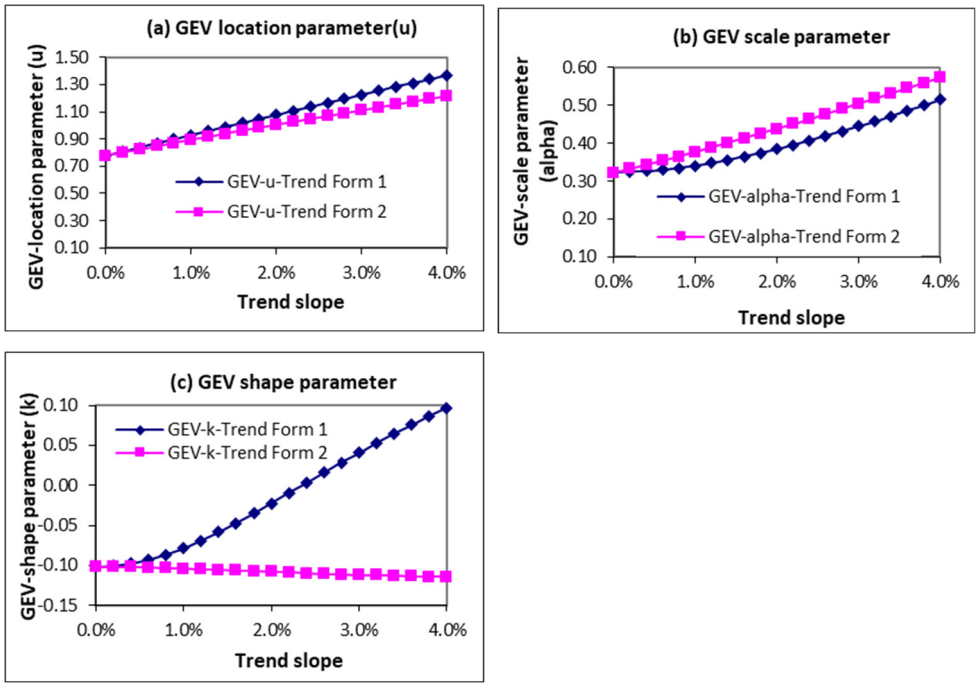

Figure 4: Comparison of the changes in regional average distribution parameters for GEV distribution

The changes in EV1 distribution parameters are similar to that of the GEV location and scale parameters [Figure 5(a) & 5(b)], i.e., both parameters increase with the increase in trend slopes in both trend forms. The increase rate in the location parameter is slightly higher in TF-1; while lesser in the scale parameter. The higher increase rate in the scale parameter is expected in TF-2, compare to TF-1, since TF-2 inflates sample variability. Table 4 presents the changes in regional average distribution parameters (GEV & EV1) for 1% trend increase for both trend forms.

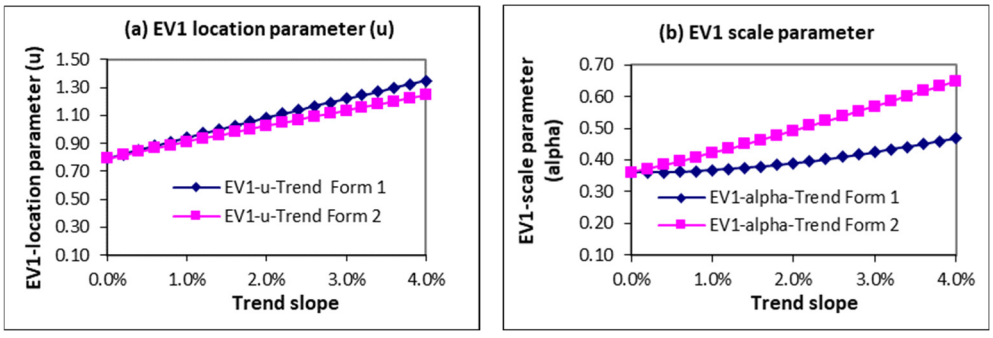

Figure 5: Comparison of the changes in regional average distribution parameters for EV1 distribution

Table 4: changes in regional average distribution parameters (GEV & EV1) for 1% trend increase for both trend forms.

Trend slope	GEV						EV1			
	u		α		k		u		α	
	TF-1	TF-2	TF-1	TF-2	TF-1	TF-2	TF-1	TF-2	TF-1	TF-2
0.0%	0.776	0.776	0.325	0.325	-0.102	-0.102	0.792	0.792	0.360	0.360
1.0%	0.929	0.894	0.341	0.377	-0.078	-0.104	0.943	0.911	0.368	0.422

3.3 Changes in Growth Curves

The results showed that growth curves in each combination of the true and fitted distributions in TF-1 get flatter and flatter as the trend slope magnitude increases [Figure 6(a) & 6(c)]. In contrast, in TF-2 growth curves in all distribution combinations get steeper and steeper with the increase in trend slopes except in the GEV-EV1 case [Figure 6(d)]. In the GEV-EV1 distribution combination growth curves get flatter with the increase in at-site trend slopes similar to TF-1 [Figure 6(b)].

Table 5 presents the estimated relative differences in growth factors (i.e., differences between the zero trend and trend condition) for a number of return periods (10-yr, 100-yr & 1000-yr) for all cases of trend forms and distribution combinations. These changes are also graphically illustrated in Figure 7. It can be seen, in the TF-1 case, growth factors decrease with the increase in trend slope while increase in trend form TF-2. The effects are larger in TF-1 than TF-2, i.e. the rate of changes in relative differences in growth curves with the increase in trend slopes are higher in TF-1 than TF-2. For example, in the TF-1 trend form, the relative differences for the 10-yr, 100-yr and 1000-yr return periods EV1-EV1 growth factors are -4.2%, -6.4%, -7.4% (decreases) respectively for a trend slope of 1%., while in TF-2 the corresponding differences are 0.7%, 1.3% and 1.7% (increases) respectively. This occurs because in TF-1, growth curves get flatter with the increase in trend slope while the opposite occurs in TF-2. The highest differences can be noticed in the GEV-GEV distribution combination followed by the EV1-GEV case in TF-1, while in TF-2, the highest differences can be noticed in the EV1-GEV distribution combination followed by GEV-EV1.

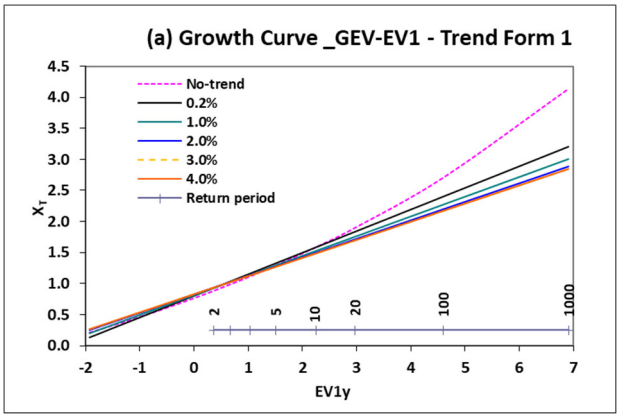

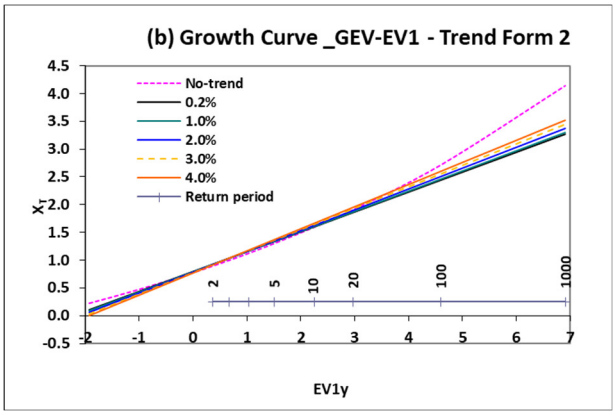

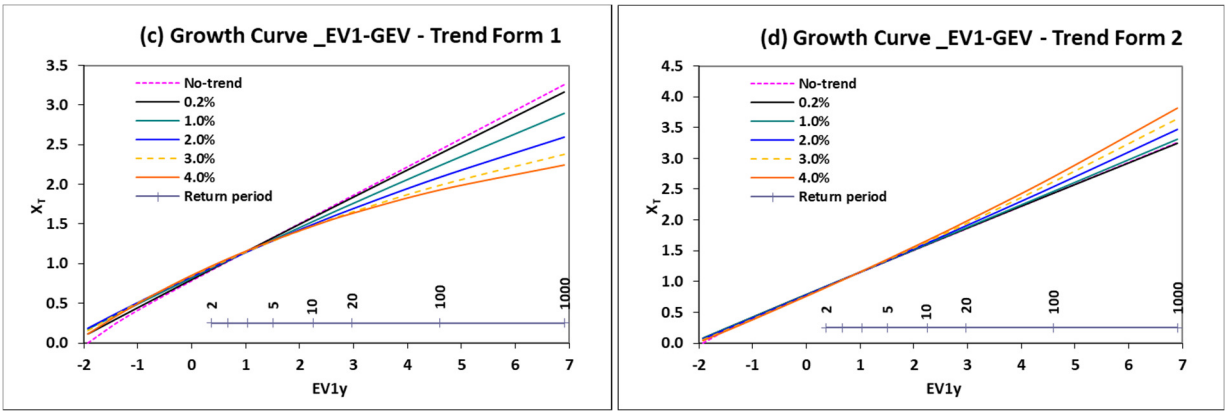

Figure 6: Changes in the growth curves with the increase in trend slopes for different true & fitted distribution combinations (left hand graphs are for TF-1 and right hand graphs are for TF-2)

Table 5: Relative differences in growth curve estimates for various combinations for true and fitted distributions under both trend forms.

Trend slope	Trend Form	F=0.90				F=0.99				F=0.999			
		GEV-GEV	GEV-EV1	EV1-EV1	EV1-GEV	GEV-GEV	GEV-EV1	EV1-EV1	EV1-GEV	GEV-GEV	GEV-EV1	EV1-EV1	EV1-GEV
0.0%	TF-1	0.1%	0.5%	0.2%	0.1%	-1.1%	-9.9%	0.5%	-0.2%	-1.9%	-21.0%	0.7%	-0.6%
	TF-2	0.3%	0.7%	0.4%	0.4%	-0.6%	-9.6%	0.8%	0.3%	-1.3%	-20.7%	1.1%	0.3%
1.0%	**TF-1**	**-4.0%**	**-3.8%**	**-4.2%**	**-4.2%**	**-10.0%**	**-15.9%**	**-6.4%**	**-8.3%**	**-14.6%**	**-27.2%**	**-7.4%**	**-11.2%**
	TF-2	**0.6%**	**1.0%**	**0.7%**	**0.7%**	**0.0%**	**-9.2%**	**1.3%**	**1.2%**	**-0.3%**	**-20.2%**	**1.7%**	**1.7%**
1.2%	TF-1	-4.5%	-4.3%	-4.8%	-4.8%	-11.5%	-16.7%	-7.3%	-9.6%	-17.2%	-28.0%	-8.5%	-13.2%
	TF-2	0.8%	1.2%	0.9%	0.9%	0.4%	-8.9%	1.6%	1.7%	0.2%	-19.9%	2.0%	2.5%
2.0%	TF-1	-5.8%	-5.8%	-6.3%	-6.4%	-17.1%	-18.8%	-9.8%	-14.3%	-26.6%	-30.1%	-11.4%	-20.4%
	TF-2	1.7%	2.1%	1.8%	1.8%	2.2%	-7.6%	3.1%	4.2%	2.8%	-18.6%	3.7%	6.4%
2.4%	TF-1	-6.2%	-6.2%	-6.8%	-7.0%	-19.4%	-19.3%	-10.5%	-16.1%	-30.5%	-30.7%	-12.3%	-23.3%
	TF-2	2.2%	2.6%	2.3%	2.3%	3.2%	-6.9%	3.9%	5.5%	4.2%	-17.8%	4.7%	8.6%
3.0%	TF-1	-6.5%	-6.5%	-7.2%	-7.4%	-22.1%	-19.8%	-11.1%	-18.3%	-35.3%	-31.1%	-13.0%	-27.0%
	TF-2	3.0%	3.4%	3.1%	3.1%	4.8%	-5.8%	5.1%	7.5%	6.2%	-16.7%	6.1%	11.8%
4.0%	TF-1	-6.7%	-6.5%	-7.2%	-7.7%	-25.3%	-19.7%	-11.2%	-20.8%	-40.7%	-31.1%	-13.1%	-31.1%
	TF-2	4.2%	4.7%	4.4%	4.3%	7.2%	-3.9%	7.2%	10.8%	9.6%	-14.8%	8.5%	17.1%

The above results suggest that trends in the records in a pooling group will have some effects on the regional growth curves. The magnitude of this effect depends on the trend forms and trend slopes. These effects result from the changes in the sample properties and distribution parameters. Regardless of the trend forms and distribution combinations, the estimated effect of the trend on the 100-year growth factor could be as large as 15.9 % for a trend slope of 1%. It can also be seen from Figure 7 that at approximately 2.4% trend slope the estimated growth factor from both GEV-GEV and EV1-EV1 distribution combinations are equal meaning that the GEV distribution takes the form of EV1 distribution (k=0) at that this trend slope.

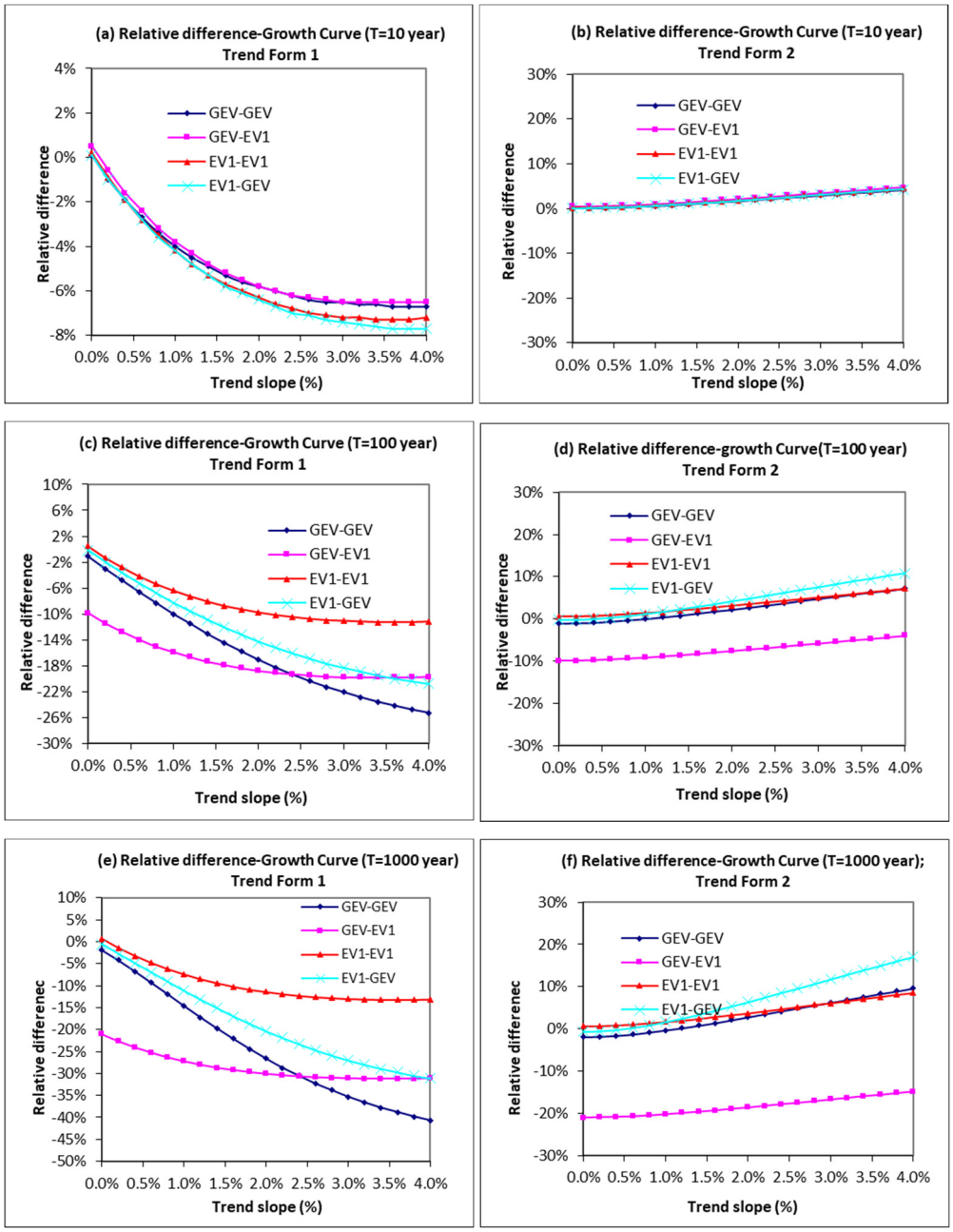

Figure 7: Comparison of the changes in relative differences in growth factors with the increase in trend slopes for different true & fitted distribution combinations (left hand graphs are for TF-1 and right hand graphs are for TF-2)

3.4 Changes in At-site Quantiles

Similar to growth curve, the changes in the at-site quantile estimates were also investigated for both trend forms. The results showed the at-site quantiles in each combination of the true and fitted distributions increase with the increase in at-site trend slope magnitudes in both trend forms with some exception in the GEV-GEV distribution combination in TF-1. In this case, for any trend slope greater than 1.2%, the estimated quantiles get smaller than the no-trend condition estimates, especially for T≥ 500 years. The increase rate is larger for the larger return periods in both trend forms.

The above changes in the quantile functions can be explained with the help of corresponding changes in growth curves and at-site sample mean with the increases in trend slopes as discussed in the sections

3.1 and 3.3. This explanation is appropriate, since the index flood method uses these two variables in estimating the at-site quantile estimates, i.e. $Q_T = Q_{mean} \times X_T$.

As was shown earlier, the at-site sample mean increases with the increase in trend slope in a linear fashion in both cases of trend forms (section 3.1). The growth curves also increase with the increase in trend slopes in the cases of TF-2. Thus, it is obvious that the quantile estimates will be increased with the increase in trend slopes under this trend form scenario. On the other hand, the growth factors decrease with the increase in trend slopes in the TF-1 scenario. However, this decrease rate is slower than the increase rate of the at-site sample mean. Thus, the quantile estimates in the case of TF-1 aslo increase with the increase in trend slopes. The differences between various true and fitted distribution combinations in the case of quantile estimation are similar to the corresponding differences in the growth curve estimates.

Table 6 presents the estimated regional average relative differences in quantile estimates for (percentage increase/decrease over the stationary condition) associated with the 10-yr, 100-yr and 1000-yr floods for various trend slopes, trend forms and true and fitted distribution combinations. These are also graphically illustrated in Figure 8. It can be seen from this figure that the quantiles estimates increase with increasing trend slopes in all trend forms and distribution combinations. In contrast to growth curve, the effect of trends on the regional estimate of at-site quantile is larger in TF-2 than TF-1, i.e. the change rates of relative differences in quantile estimates with the increase in trend slopes are higher in TF-2 than TF-1. This occurs because in TF-1 growth curves get flatter (or growth factors decrease) with increasing trend slope while the opposite occurs in TF-2. For example, in the TF-1 case, the relative differences for the 10-yr, 100-yr and 1000-yr EV1-EV1 quantile estimates are 10.7%, 8.1% and 6.9% respectively for a trend slope of 1%., while in TF-2 the corresponding differences are 16.3%, 17.0% and 17.4% respectively.

The differences between the various distribution combinations are imperceptible for the smaller return period for both trend forms. However, these become significant with the increase in return periods. The highest differences can be noticed in the EV1-EV1 distribution combination followed by the GEV-EV1 case in TF-1, while in TF-2, the highest differences can be noticed in the EV1-GEV distribution combination followed by the GEV-EV1 and GEV-GEV combinations.

It can also be seen in the Figure 8 that the difference in quantile estimates for the distribution combinations of GEV-GEV and GEV-EV1 are almost same at the trend slope of 2.4%. The means that the at this trend slope the GEV distribution takes the form of EV1 distribution i.e. the shape parameter becomes near to zero. Any further increase in trend slopes, the shape parameter increases, thus the quantile functions become concave upward and therefore the quantile estimates at the larger return periods become smaller than the true estimates.

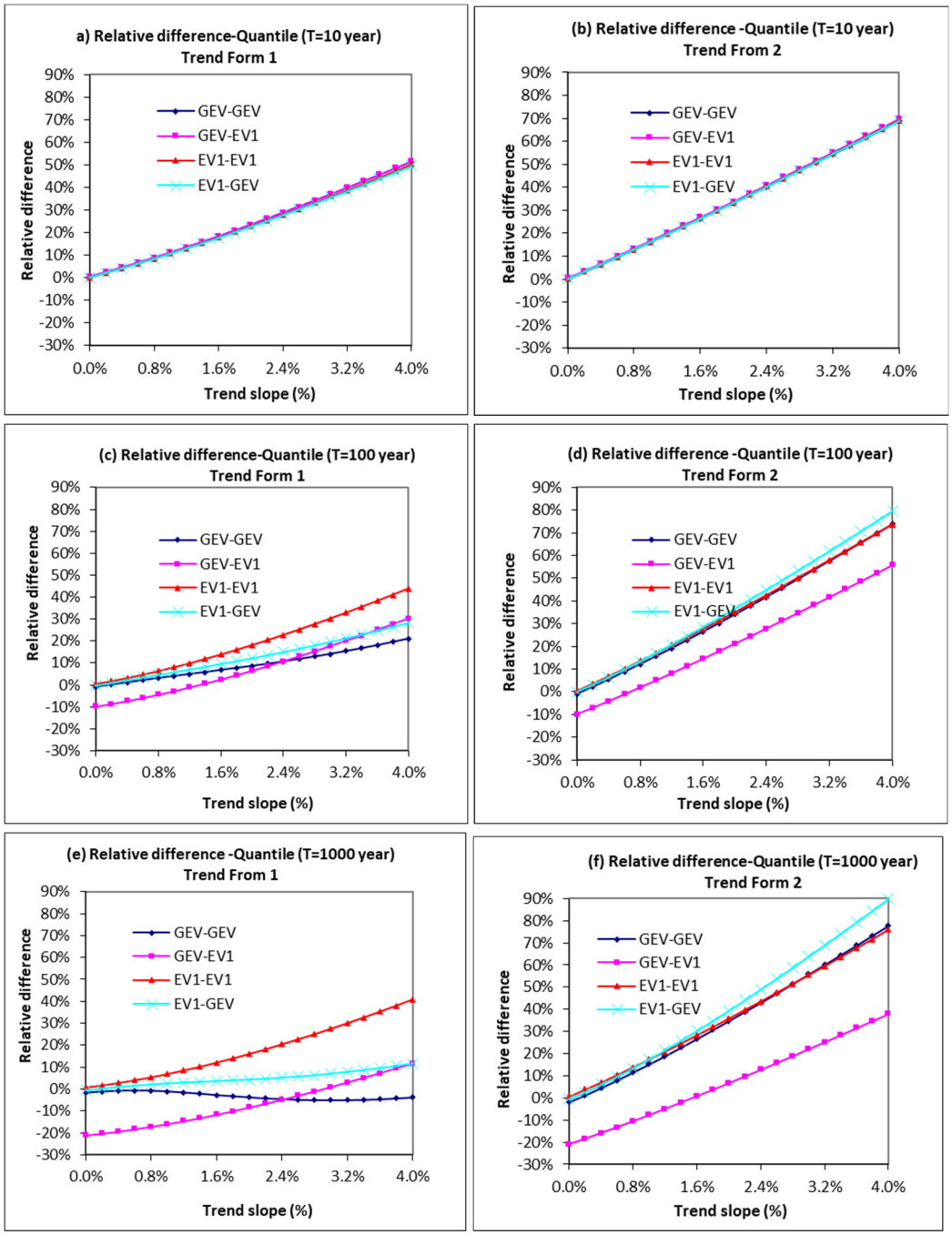

Figure 8: Comparison of the regional average relative differences in quantile estimates for different combinations of true and fitted distributions

The above results suggest that trends in the records in a pooling group will have some effects on the regional estimates of at-site quantiles. The magnitude of this effect depends on the trend forms and trend slopes. These effects result from changes in sample properties and distribution parameters. Regardless of the trend form and distribution combinations, the estimated effect of the trend on the 100-year growth factor could be as large as 17 % (increase) for a trend slope of 1%.

Table 6: Relative differences in regional average at-site quantile estimates for various combinations for true and fitted distributions under both trend forms

Trend slope	Trend Form	F=0.90				F=0.99				F=0.999			
		GEV-GEV	GEV-EV1	EV1-EV1	EV1-GEV	GEV-GEV	GEV-EV1	EV1-EV1	EV1-GEV	GEV-GEV	GEV-EV1	EV1-EV1	EV1-GEV
0.0%	TF-1	0.1%	0.5%	0.2%	0.1%	-1.0%	-9.9%	0.5%	-0.2%	-1.8%	-21.0%	0.7%	-0.6%
	TF-2	0.1%	0.5%	0.2%	0.1%	-1.0%	-9.9%	0.5%	-0.2%	-1.8%	-21.0%	0.7%	-0.6%
1.0%	**TF-1**	**10.9%**	**11.1%**	**10.7%**	**10.6%**	**4.0%**	**-2.9%**	**8.1%**	**5.9%**	**-1.2%**	**-15.9%**	**6.9%**	**2.6%**
	TF-2	**16.3%**	**16.7%**	**16.3%**	**16.3%**	**15.6%**	**4.9%**	**17.0%**	**16.9%**	**15.2%**	**-7.8%**	**17.4%**	**17.4%**
1.2%	TF-1	13.3%	13.5%	13.0%	12.9%	4.9%	-1.2%	9.9%	7.2%	-1.7%	-14.6%	8.5%	3.0%
	TF-2	19.6%	20.1%	19.7%	19.6%	19.1%	8.1%	20.5%	20.7%	18.9%	-5.0%	21.0%	21.6%
2.0%	TF-1	23.4%	23.4%	22.7%	22.5%	8.6%	6.4%	18.2%	12.3%	-3.8%	-8.4%	16.0%	4.3%
	TF-2	33.3%	33.8%	33.4%	33.3%	34.0%	21.1%	35.0%	36.5%	34.8%	6.7%	35.9%	39.4%
2.4%	TF-1	28.7%	28.7%	27.9%	27.7%	10.7%	10.7%	22.8%	15.1%	-4.6%	-4.9%	20.4%	5.2%
	TF-2	40.2%	40.8%	40.4%	40.3%	41.7%	27.8%	42.5%	44.8%	43.0%	12.7%	43.6%	49.0%
3.0%	TF-1	36.9%	37.0%	36.0%	35.6%	14.1%	17.6%	30.2%	19.7%	-5.1%	0.9%	27.5%	7.0%
	TF-2	50.9%	51.5%	51.1%	51.0%	53.6%	38.1%	54.0%	57.6%	55.8%	22.1%	55.5%	63.9%
4.0%	TF-1	51.2%	51.5%	50.3%	49.5%	21.1%	30.1%	43.8%	28.3%	-3.9%	11.6%	40.8%	11.6%
	TF-2	68.9%	69.7%	69.2%	69.0%	73.8%	55.7%	73.6%	79.6%	77.7%	38.0%	75.9%	89.8%

4. Unrealistic Results for GEV Distribution

In the trend form TF-1, for any trend slope greater than 1.2%, the estimated quantiles from GEV-GEV distribution were found to be smaller than the no-trend condition estimates, especially for T≥500-years. Thus, the GEV distribution gives unrealistic results for the larger return periods. This could be occurring due to its very strong relationship with the shape parameter and also due to estimating these extremely larger return period quantiles from a comparatively shorter pooling group size (450 station-years). A sensitivity analysis for various pooling group sizes showed that in order to get a realistic estimate for a 1000-year return period quantile for any trend slope of 1%, at least 200 years of record length would be required at each of the sites in the region which is equivalent to a pooling group size of 3000 station-years (i.e. pooling group size should be at least three times of return period-3T). Figure 9(a) and Figure 9(b) illustrate the estimated quantile functions for site 1 for both 450 station-years and 3000 station-years pooling groups respectively.

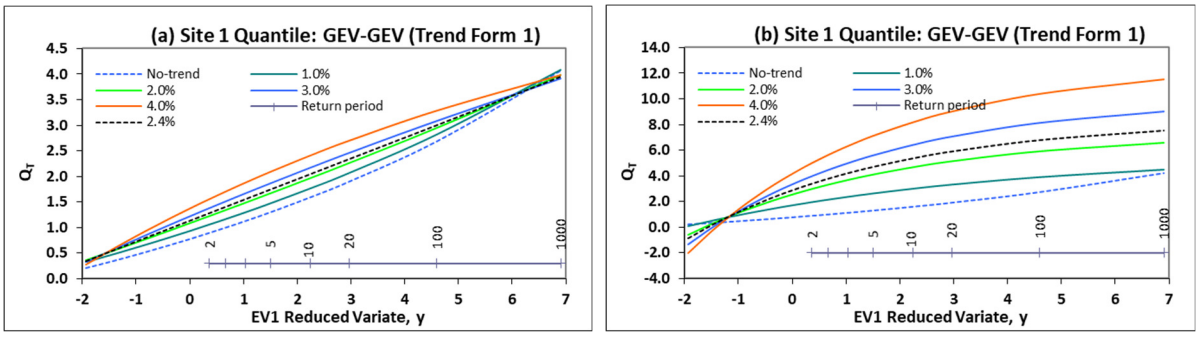

Figure 9: Quantile functions for the 450 and 3000-station years Figure (a) & (b) respectively] for TF-1 and GEV-GEV distribution combination (Site 1)

5. CONCLUSIONS AND RECOMMENDATIONS

The simulation results show that trends in the data series cause changes in the sample properties and distribution parameters. The impact of the change depends on the form and magnitude of trend slopes and type of true distribution. TF-1 was found to generally flatten growth curves, while TF-2 has the opposite effect. These changes can be as large as 16% at T=100 and trend slope of 1%. Trend effect on quantiles is generally positive, largely caused by an increase in the index-flood, with increases up to 17% at T=100 and 1% trend slope. This suggests, the current practice of adding 20% allowance in the design flow estimate, to cater for the future climate change effect, just about accounts for this.

Some unrealistic results emerged in the GEV-GEV simulation case, where large return period floods showed a decrease caused by the estimated GEV k value being (unexpectedly) positive when estimated from the data containing trends. The performance of the two-parameter EV1 distribution in fitting a GEV sample with a higher trend was found to be better than fitting a GEV distribution. EV1 distribution is found to be safer than GEV distribution in the presence of trends, particularly when larger return period quantile estimates are required, i.e. EV1 distribution is more robust in this case.

Until now no acceptable procedure has been developed and/or adopted to deal with the non-stationary properties of data series. Therefore, the findings of the current study could help hydrologists/engineers to make an allowance in the estimated design flood using the conventional statistical procedure. However, in order to accomplish this further research on this should be carried out. This should include: (i) updating the FSU trend test results; (ii) determination of the magnitude and form of trend present in the Irish Rainfall and Annual Maximum Flood Series; and (iii) subsequently developing a practical procedure for estimating the design flood flows when trends/non-stationarity are present in the data series. Trend slopes in the historical data series can be estimated from the Theil (1950) and Sen (1968) proposed method or from the regression slope method. These methodologies are recommended for use within future studies.

ACKNOWLEDGEMENTS:

Data for this study were obtained from EPA/ESBI, OPW and Met Eireann. The authors would like to thank University of Galway and RPS Consulting Engineers for their support in undertaking this research work.

6. REFERENCES

Adamowski, K., Bocci, C., 2001. Geostatistical regional trend detection in river flow data. Hydrological Processes 15, 3331–3341.

Arnell, N. 2006. The implication of climate change from hydrological regimes and water resources; An overview. Irish National Hydrology Seminar, 2006. pp. 1-7.

Anrnell, N.W. and Gabrielle, S., S., 1985. Regional flood frequency analysis with the two- component extreme value distribution: An assessment using computer simulation experiments. Workshop on combined efficiency of direct and indirect estimations for point and regional flood prediction, Perugia, Italy, December.

Burn, D.H. and M.A. Hag Elnur. 2002. Detection of hydrologic trend and variability. J. Hydrol. 255: 107-122.

Cox, D.R., Isham, V.S. and Northrop,P.J., 2002. Floods: some probabilistic and statistical approaches. Philosophical Transactions of Royal Society London, Series A vol. 360, 1389- 1408.

Cunderlik, J.M. and D.H. Burn. 2002. Local and regional trends in monthly maximum flows in southern British Columbia. Can. Water Resour. J. 27: 191-212.

Cunderlik, J.M. and D.H. Burn. 2003. Non-stationary pooled flood frequency analysis. Journal of Hydrology 276 (2003) 210-223.

Cunnane, C., 1988. Methods and merits of regional flood frequency analysis. Journal of Hydrology, 100, 269-90.

Cunnane, C., 1989. Statistical Distributions for flood frequency analysis. WMO., Operational Hydrology Report No. 33. WMO. No. 718.

Das, S., Cunnane, C., 2011. Examination of homogeneity of selected Irish pooling groups. Hydrol. Earth Syst. Science, 15, 819-830.

Duckstein, L., Bobee, B. and Bogardi, I. (1987). Bayesian forecasting of hydrologic variables under changing climatology. In The Influence of Climate Change and Climatic Variability on the Hydrologic Regime and Water Resources, Proceedings of the Vancouver Symposium, IAHS Publication 168, Aug. 1987, pp. 301–311.

Hosking J.R.M, Wallis, J.R., and Wood, E.F., 1985a. An appraisal of the regional flood frequency procedure in the UK Flood Studies report, Hydrol. Sc. J., 30(1), 85-109.

Hosking, J.R.M and Wallis, J.R., 1993: Some statistics useful in regional frequency analysis. Water Resources research, 29, 271-281, 1993.

Hosking, J.R.M. and J.R. Wallis , 1997: Regional frequency analysis: An approach based on L- moments. Cambridge University Press.

Hosking, J.R.M., 1990: L-moments: Analysis and estimation of distributions using linear combinations of order statistics. Journal of the Royal Statistical Society, B 52(1): 105-124.

Hosking, J.R.M., Wallis, J.R. and Wood, E.F. (1985b). Estimation of the generalised extreme value distribution by the method of probability – weighted moments. Technometrics, 27, 251- 261.

IPPC, 1996. Climate change 1995. The second IPC Scientific assessment. In: Houghton, J.T., Meria Filho, L.A., Callender, B.A. (Eds). Intergovernmental Panel on Climate Change. Cambridge University Press, Cambridge, UK.

IPPC, 2001. Climate Change 2001. Impacts, Adoption and Vulnerability. Contribution of Working Group II to the Third Assessment of the IPCC on Climate change. Cambridge University Press, Cambridge, UK.

IPPC, 2001. Climate Change 2001. The Scientific Basis. Contribution of Working Group I to the Third Assessment Report of IPCC on Climate change. Cambridge University Press, Cambridge, UK.

IPCC, 2007. Climate Change 2007. The Physical Science Basis. Contribution of Working Group I to the Fourth Assessment Report of the Intergovernmental Panel on Climate Change (IPCC).

IPCC, 2007, Climate change 2007: Synthesis report. Contribution of Working Groups I, II and III to the Fourth Assessment Rep., Geneva.

IPCC, 2021, Climate Change 2021: The Physical Science Basis. Contribution of Working Group I to the Sixth Assessment Report of the Intergovernmental Panel on Climate Change.

Jain, S., Lall, U., 2001. Floods in changing climate: does the past represent the future? Water Resources Research 37 (12) 3193-3205.

Kendall, M,G., Stuart, A., Ord, J.K. 1983. The Advanced Theory of Statistics, Volume 3. Griffin, London.

Khaliq, M.N., Ouarda, T.B.M.J., Ondo, J.-C., Gachon, P., Bobée, B., 2006. Frequency analysis of a sequence of dependent and/or non-stationary hydrometeorological observations: a review. J. Hydrol. 329, 534–552.

Kiely, G., 1999. Climate change in Ireland from precipitation and streamflow observations. Advances in Water Resources 23(1999) 141-151.

Kundzewicz, Z. W. & Robson, A. (eds) (2000) Detecting Trend and Other Changes in Hydrological Data. World Climate Programme—Water, World Climate Programme Data and Monitoring, WCDMP-45, WMO/TD no. 1013. World Meteorological Organization, Geneva, Switzerland.

Lettenmaier, D.P., 1976. Detection of trend in water quality data from records with dependent observations. Water Resour. Res. 12 (5), 1037–1046.

Mandal, U. and Cunnane, C., 2011. Studies in low and flood flow estimation for Irish river catchments. PhD thesis, College of Engineering and Informatics, NUI Galway, 282pp

NORTH, M. (1980). Time-dependent stochastic model of floods. J. Hyd. Div., 106: 649–665.

OPW Flood Studies Update Programme, Work-Package 2.2 " Flood Frequency Aanalysis" - Analysis of Trend in Irish Annual Maximum Flood Series, July 2009, National University of Ireland, Galway, Department of Engineering Hydrology.

Pilon, P.J. and S. Yue. 2002. Detecting climate-related trends in streamflow data. Water Sci. Technol. 8(45): 89-104.

Porporato, A., Roidolfi, L., 1998. Influence of week trends in exceedance probability. Stochastic Hydrology and Hydraulics 12, 1-14.

Sen, P.K., 1968. Estimates of the regression coefficient based on Kendall's tau. Journal of the American Statistical Association 63, 1379–1389.

Strupczewski, W.G., Kaczmarek, Z., 2001. Non-stationary approach to at-site frequency modelling II. Weighted least squares estimation. Journal of Hydrology 248, 143-151.

Strupczewski, W.G., Singh, V.P., Feluch, W., 2001a. Non-stationary approach to at-site flood frequency modeling I. Maximum likelihood estimation. J. Hydrol. 248, 123–142.

Strupczewski, W.G., Singh, V.P., Mitosek, H.T., 2001b. Non-stationary approach to at-site flood frequency modeling III. Flood analysis of Polish rivers. J. Hydrol. 248, 152–167.

Theil, H., (1950): "A rank-invariant method of linear and polynomial regression analysis", Proceedings of Koninklijke Nederlandse Akademie van Wetenschappen A.53: 1397–1412

Yue, S., P.J. Pilon, B. Phinney and G. Cavadias. 2002b. The influence of autocorrelation on the ability to detect trend in hydrological series. Hydrolog. Process. 16(9): 1807-1829.

Yue, S., P.J. Pilon, G. Cavadias and B. Phinney. 2002a. Power of the Mann-Kendal and Spearmans rho tests for detecting monotonic trends in hydrological series. J. Hydrol. 259: 254-271.